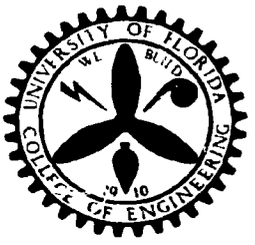

ENGINEERING AND INDUSTRIAL EXPERIMENT STATION

College of Engineering

University of Florida

Gainesville

ORO-3262-58

DEFORMATION PROCESSES IN REFRACTORY METALS

Progress Report

L. P. Beckerman, I. G. Watson

and R. E. Reed-Hill

Department of Materials Science and Engineering
University of Florida
Gainesville, Florida 32611

December 1, 1977 - November 30, 1978

Prepared for the Department of Energy

under Contract No. EY-76-S-05-3262

PROGRESS REPORT

A. Overall Project:

1. a) Paul G. Watson

Task - Dynamic strain-aging and slow strain-rate embrittlement in niobium due to oxygen and nitrogen.

Degree goal - Master of Science (Metallurgy)

Matriculation date - March 1979

b) Linda P. Beckerman

Task - Static strain-aging under stress of vanadium containing oxygen.

Degree goal - Doctor of Philosophy (Metallurgy)

Matriculation date - September 1979

c) Francisco J. M. Boratto

Task - Measurement of the diffusion coefficients of oxygen and nitrogen in niobium, vanadium and tantalum.

Degree goal - Doctor of Philosophy (Metallurgy)

Matriculation date - December 1977

2. Publications:

1. F.J.M. Boratto and R.E. Reed-Hill, "Oxygen and Nitrogen Diffusion in Vanadium," Scripta Met., 1977, vol. 11, pp. 1107-12.
2. W.R. Cribb and R.E. Reed-Hill, "The Initial Development of a Yield Point Due to Carbon in Nickel 200 During Static Strain-Aging," Met. Trans. A, 1978, vol. 9A, pp. 887-90.
3. J.R. Donoso, A.T. Santhanam and R.E. Reed-Hill, "Slow Strain-Rate Embrittlement in Metals," Spec. Vol., pp. 515-33, Proc. 2nd Int. Conf. Mech. Beh. Mets., ASM, Metals Park, Ohio, 1978.

4. J.R. Donoso, P.G. Watson and R.E. Reed-Hill, "The Effect of Dynamic Annealing on Dynamic Strain-Aging Phenomena in Commercial Purity Titanium," accepted for publication in Met. Trans. A.

5. F.J.M. Boratto and R.E. Reed-Hill, "Oxygen and Nitrogen Diffusion in Tantalum," Scripta Met., 1978, vol. 12, pp. 313-18.

6. J.R. Donoso, P.G. Watson and R.E. Reed-Hill, "Author's Reply to Discussion of Met. Trans. A, 1977, vol. 8A, pp. 945-48," Met. Trans. A, 1978, vol. 9A, p. 742.

7. J.R. Donoso, P.G. Watson and R.E. Reed-Hill, "Some Further Observations Relative to Static Strain-Aging in Commercial Purity Titanium," submitted for publication to Met. Trans. A.

3. Result of Major Significance

a) Scientific Importance:

While it has been known for sometime that aging under stress may increase the magnitude of the yield point return during static strain-aging,[1-4] the effect of the aging stress level on the yield point return has not been studied in detail. The development of an electronic load maintaining device for our Instron machine has made studying the effect of stress on the aging response feasible. While to this date this equipment has only been employed to study the phenomena associated with the initial stages of aging due to oxygen in vanadium, where aging is due to Snoek ordering of the interstitial around the dislocation, this limited study has given some very interesting results. The first is the observation that the magnitude of the yield point return, $\Delta\sigma$, maximizes

at an aging stress equal to 0.92 σ_f where σ_f is the prestrain flow stress at a strain-rate of $6.7 \times 10^{-5} s^{-1}$. Above this aging stress the value of $\Delta\sigma$ falls sharply as may be seen in Fig. 1. Below 0.92 σ_f the yield point return drops more slowly falling to about one third of its value at 0.10 σ_f which may be taken as a measure of its value for aging at zero stress. It is important to note that a sizeable fraction of this zero aging stress yield point increment may be due to the Haasen and Kelly[5] unloading yield point effect. Another very important observation is that for aging at a stress giving the maximum yield point return, aging occurs while the specimen is undergoing strain at a finite rate. This strain-rate is only about two and a half orders of magnitude smaller than that at which the specimen was prestrained. This implies that the maximum yield point return occurs under a condition where the mobile dislocations existing during prestrain are still mobile. In other words, aging under stress occurs essentially under dynamic conditions and has to be closely related to dynamic strain-aging. However, this new form of test can be performed under better controlled conditions than those existing in a simple tensile test and should, we feel, yield information allowing the complicated phenomena associated with dynamic strain-aging to be more easily understood.

b) Relevance to Energy Technology:

The efficient production of energy from either fossil or nuclear fuels requires material components to be subjected to elevated temperatures. In these operating temperature ranges steels, titanium, zirconium

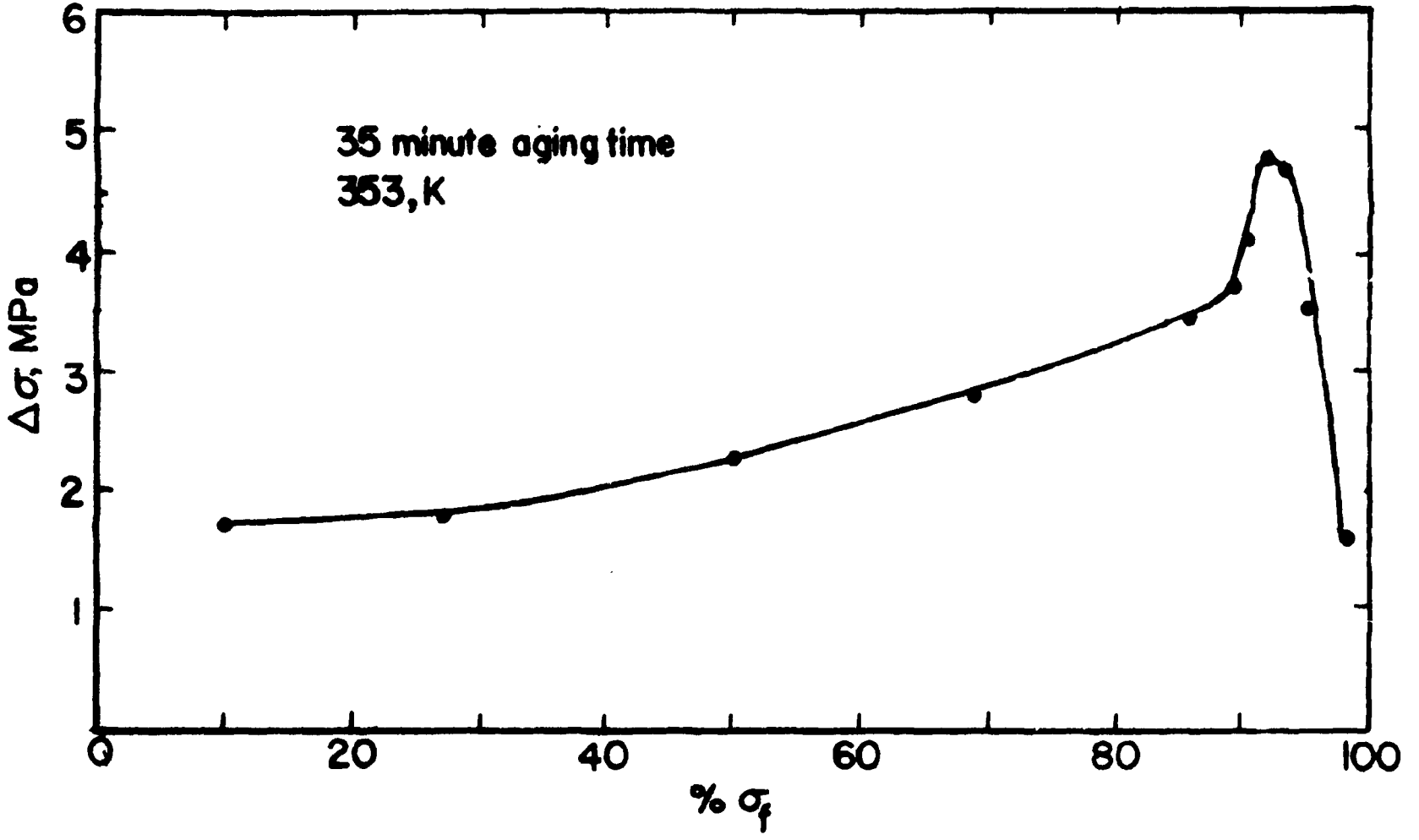

Figure 1. Effect of stress on the yield point return observed for a constant aging time, 35 minutes. Stress levels range from 10% to 98% of the flow stress.

and refractory metals such as niobium, vanadium and tantalum all become subject to dynamic strain-aging and slow strain-rate embrittlement due to the presence of interstitial solutes such as oxygen, nitrogen and carbon. Intelligent use of these metals requires that we thoroughly understand how the interstitial solutes develop these two classes of phenomena that strongly influence the mechanical properties of the refractory metals in their useful temperature ranges. We believe that this new technique can significantly yield data that will aid our understanding of these phenomena.

B. Task Summaries:

Task I - Dynamic Strain-Aging and Slow Strain-Rate Embrittlement of Niobium Due to Oxygen and Nitrogen - Paul G. Watson

1. Objectives - To obtain a characterization of the embrittlement and dynamic strain-aging phenomena in terms of strain-rate, temperature and composition parameters. This work represents an extension of the work originally performed by Donoso[6] using wire specimens. Presently, standard ASTM threaded end specimens are being employed in order to improve the reliability of the data. In the past year over 50 tests have been performed on material of one composition (0.7 at.% O, 0.05 at.% N) employing three strain-rates covering the temperature range from 300 to 1000 K.
Salient aspectives of progress - (1) At an intermediate strain-rate ($\sim 10^{-4}s^{-1}$), two distinct slow strain-rate embrittlement minima were observed centered near 530 and 770 K, possibly due to the presence respectively of oxygen and nitrogen. Decreasing the strain-rate resulted

in a single, more extensive ductility minimum. (2) Two distinct dynamic strain-aging work hardening peaks were also observed. (3) A correlation between the dynamic strain-aging work hardening peaks and the slow strain-rate embrittlement phenomena was observed. A sharp decrease in ductility was observed to occur about 50 K below both of the work hardening peaks at a strain-rate of $3.3 \times 10^{-5} s^{-1}$. (4) A scanning electron microscope study of the fractured specimens also showed a number of morphological changes in the fracture modes which correlate with changes in the dynamic strain-aging work hardening behavior. For example, the fracture transition that occurs some 50 K below the lower temperature work hardening peak involves a shift, on increasing the temperature, from ductile microvoid coalescence to brittle transgranular fracture. This correlation strongly suggests that the onset of brittle fracture is closely associated with the dynamic strain-aging annomalous work hardening behavior.

2. Relation of progress to:

(a) Earlier progress - The present work on niobium-oxygen embrittlement is a continuation of work begun several years ago on this contract. At that time, an investigation was instituted into the feasibility of observing a slow strain-rate embrittlement regime due to interstitials other than hydrogen. Because of its high recovery temperature and relatively fast oxygen diffusivity the niobium-oxygen system was chosen for the initial survey. This survey used oxygen doped niobium wires and produced data which clearly showed a ductility minimum that increased in severity with increasing oxygen concentration and decreasing strain-rate. However, it proved difficult to reliably obtain other tensile properties from the wire data. For this reason, research was instituted that involved

increasing the size of the tensile specimens while maintaining oxygen uniformity across the gage section and a uniform and reasonable grain size. This task was initiated last year and led to the initial survey of the system presented in this report.

(b) Other tasks - At present, the major goal of this program is to investigate the interaction between interstitial solutes and mechanical properties of refractory metals of significance in energy production. As such, this study of an oxygen induced embrittlement of niobium directly supports this effort.

(c) Additionally, this study benefits from the ongoing strain-aging investigations in vanadium involving aging under stress which is throwing light on the interaction of interstitials and dislocations involving both Schoeck-Seeger[7] and Cottrell[8] pinning mechanisms and in particular the role that these mechanisms play in dynamic strain-aging in BCC refractory metals.

Task II - Static Strain-Aging Under Stress of Vanadium Containing Oxygen - Linda P. Beckerman

1. Objectives - To make a detailed study of the effect of stress on static strain-aging in vanadium containing oxygen using a testing technique capable of maintaining a fixed load on the specimen during aging. The technique allows the strain occurring during the aging period to be measured, thus making possible an estimate of the magnitude of the work hardening occurring during aging. At the same time the strain-rate at

any time during the aging treatment can also be evaluated.

Salient aspects of progress - In the early stages of aging normally associated with Snoek ordering of interstitials in the strain fields of the dislocations, it has been observed for specimens deformed at a strain-rate of $6.7 \times 10^{-5} s^{-1}$ at 353 K,

(a) Aging under stress occurs under a measurable strain-rate during aging to stress levels below 0.88 σ_f where σ_f is the prestrain flow stress at 9% strain. (b) Within the aging stress level between 0.86 σ_f and 0.98 σ_f the average strain-rate over a 35 minute aging period follows a power law with respect to the aging stress. See Fig. 2. The strain-rate sensitivity, as defined by the relation $n = d \ln \sigma / d \ln \dot{\epsilon}$, was 0.017 which is in good agreement with the value of n measured by a change in strain-rate experiment by Bradford and Carlson[9] for vanadium at 353 K. (c) The yield point for specimens, aged 35 minutes, when plotted as a function of aging stress passes through a sharp maximum at 0.92 σ_f as may be seen in Fig. 1 on page 4 where the average strain-rate is only about 2.5 orders slower than the nominal prestrain flow stress. (d) While it is too early in the present investigation to draw firm conclusions concerning the mechanism of aging under stress, some speculations on the above results are probably in order:

(1) Aging under stress apparently involves aging of the mobile dislocations. This would be consistent with Snoek ordering or aging of dislocations waiting for thermal activation in order to pass through penetrable obstacles.

(2) The decrease of the yield point above 0.92 σ_f, see Fig. 1, could

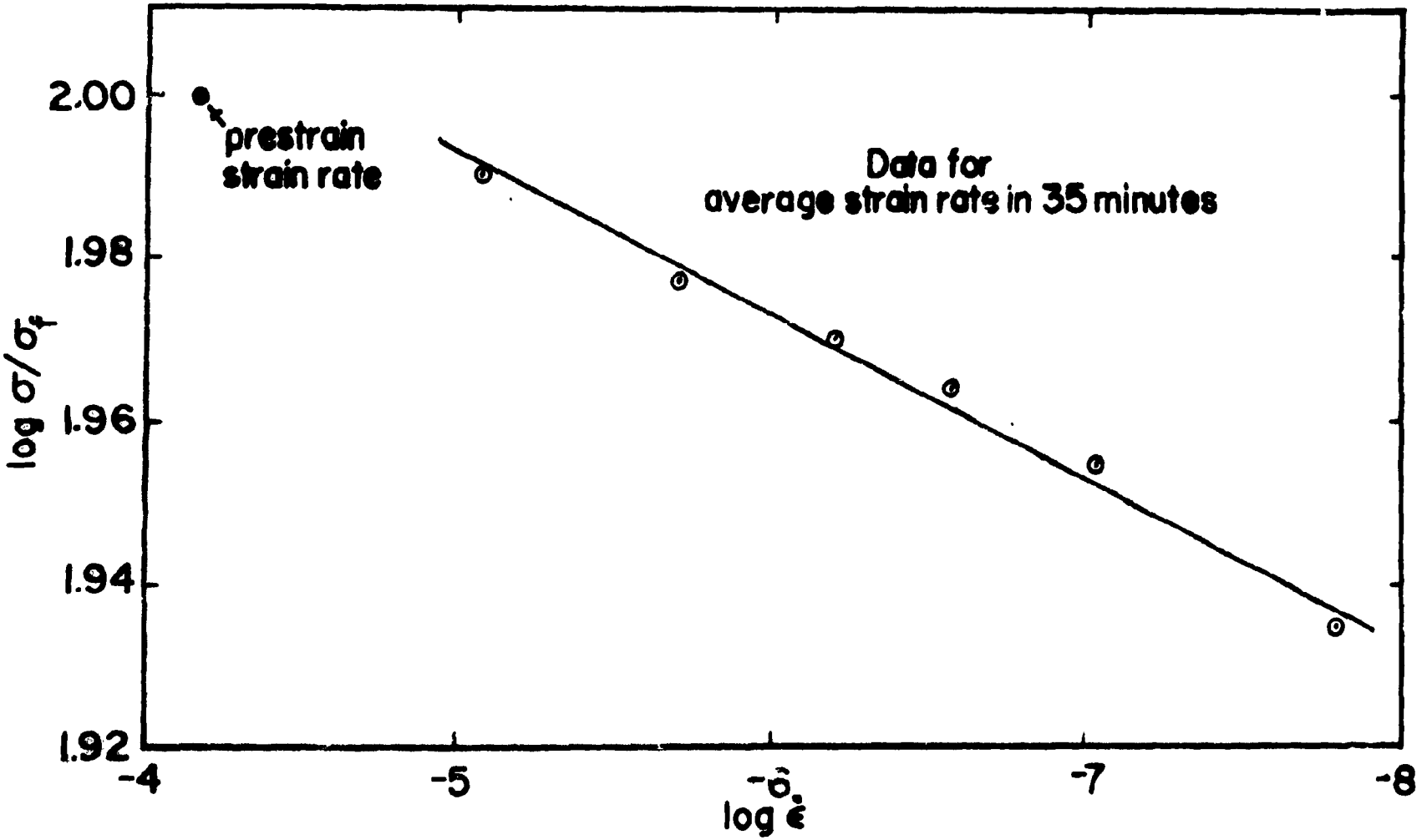

Figure 2. The average strain-rate over a 35 minute aging period is seen to follow a power law with respect to the aging stress.

be due to a decrease in the degree of aging due to the fact that the waiting time at an obstacle decreases with increasing stress (strain-rate) as the aging stress approaches the prestrain flow stress.

(3) The decrease in the yield point below 0.92 σ_i may be due to dislocation rearrangements as the aging stress approaches and falls below the internal stress. At high stress levels it is to be expected that the mobile dislocations will be pressed against the obstacles controlling their motion. Under these conditions the aging of the dislocations could be expected to produce a maximum effect on the yield stress or yield point. Lowering the stress should allow an increasing degree of relaxation of the dislocations back away from the obstacles. Under these conditions the aging of a dislocation due to Snoek ordering could occur while a dislocation was effectively removed from the field of influence of the obstacle. On reloading the dislocation could then escape from its ordered atmosphere before having to pass through the obstacle. This, of course, would occur before macro-yielding or in the region of micro-strain region and, depending on the degree of relaxation, should tend to decrease the size of the observed yield point.

2. Relation of progress to:

(a) Earlier progress - This is a newly devised project.

(b) Other tasks - This task is designed to support the other primary task of this project. Knowledge obtained with respect to the nature of the aging process gained under the condition of aging under stress should be helpful in obtaining a better understanding of the phenomena of dynamic

strain-aging. The fact that this task is being performed using vanadium specimens and the other using niobium should have only a minor effect on the final conclusion.

(c) Overall project goals - This task conforms to the general goals of the project which are to study the influences of factors such as deformation twinning, dynamic strain-aging, dynamic recovery and slow strain-rate embrittlement that cause aberrations in the normal deformation processes of metals. Factors which are often ignored in the theoretical analyses of plastic deformation.

3. This is a new task.

Task III - Measurements of the Diffusion Coefficients of Oxygen and Nitrogen in Niobium, Vanadium and Tantalum - Francisco J. M. Boratto

1. Objectives - All of the objectives of this task were completed in this past year and the results of this task have appeared in four publications. An improved torsion pendulum was used which could be modified to make elastic after-effect measurements. All data were analyzed with the aid of a non-linear least squares computer optimization program. The data thus obtained were then correlated with existing data in the literature. An important result of this work was the conclusion that in niobium, vanadium and tantalum, nitrogen and oxygen apparently prefer to occupy octahedral sites in the host metals.

2. Relation of progress to:

(a-c) Accurate values for the diffusion coefficients of nitrogen and oxygen in niobium, vanadium and tantalum are essential for our study of slow strain-rate embrittlement and dynamic strain aging. Boratto's results are turning out to be very useful in achieving the overall goals of this project.

3. Statement of new or modified task objectives: This task is completed.

Task IV - Inactive Tasks:

There are two other tasks that were being worked upon at the beginning of this past year. Work has been discontinued on these two in favor of an accelerated effort on the tasks listed under I and II above.

The first of these is the work of Paul Watson involving a study of static strain-aging in the niobium-hydrogen-oxygen system. In this case, while early work involving specimens prepared from one heat of Marz grade niobium showed a strong influence of hydrogen on the energetics of the oxygen yield point in confirmation of Wilcox and Huggins earlier data, later specimens from similar heats of Marz niobium showed essentially no effect. While this presents an interesting problem, it was felt that continuing this work could not be justified on the basis of the costs involved in relation to the results that might be obtained.

Similarly the work of Linda Beckerman involving the relation of slow strain-rate embrittlement to dynamic strain-aging in the hydrogen-vanadium system was also found to be in an area where the efforts would be much less economical that where her current efforts are being expended.

C. Discussion of Progress on Task I

Introduction

Niobium and niobium based-alloys show great promise of energy related applications because of their retention of strength at high temperatures, low thermal neutron cross-section and corrosion resistance in liquid metal systems. However, these properties, and in particular the mechanical properties, can be deliteriously affected by varying levels of impurities which may enter the material during its refining, fabrication or use. This section of the report examines the results of an on-going investigation into the embrittlemen phenomena which occur when oxygen-doped niobium tensile specimens are tested between 300 and 1000 K. At the same time correlations between the embrittlement phenomena and dynamic strain-aging are being sought.

Experimental Procedure

VP grade 6.35 mm diameter, niobium rods from the Materials Research Corporation were employed in this investigation. A nominal analysis for this material is given in Table 1. Oxygen was inserted into this material by swaging the rods to 3.96 mm diameter and then cutting them into 34.9 mm lengths. Four of these lengths were then placed in 15.9 mm diameter niobium tubes containing 6.0 gm of Nb_2O_5 powder. The ends of each tube were then fusion welded shut to form a closed packet. The packet was then placed in a tube furnace and, under an argon atmosphere, heated to 1153 K for 6 1/2 hours. The rod sections were then removed from the packet, lightly etched and homogenized in a dynamic vacuum at 1273 K for 18 hours. The doping procedure was proposed by F. N. Rhines, and

TABLE 1

VP Niobium

Before oxygen doping

Element	Content (wt. ppm)
C	25
O	50
N	15
H	15
others	935

After oxygen doping

Element	Content (wt. ppm)
O	1290
N	116

has the advantage that it permits alloying to occur without the formation of non-adherent flaking scales. From these rod sections tensile specimens were machined with a 2.54 mm gage diameter and a 10.16 mm gage length. To improve specimen alignment and serve as a check on the uniformity of oxygen content among a number of specimens, each specimen was pulled to $\sim$ 0.5% strain at room temperature, and the stress levels at this strain were compared. Finally, each specimen was annealed at 1393 K for 20 minutes to recover this strain increment. At this point the tensile specimens, with a mean lineal grain boundary intercept of $\sim$ 70 μm and an oxygen level of $\sim$ 0.75 at.%, were ready for tensile testing.

A number of methods were available to check the oxygen content (and the nitrogen content) of the final material. Vacuum fusion analyses were utilized while designing the doping procedure, in order to separately determine oxygen and nitrogen concentrations introduced while varying the oxidizing and homogenizing periods and temperatures. In addition, vacuum fusion analyses were used to insure proper calibration of the published interstitial concentration-DP hardness relation. After the doping procedure had been set up, regular checks on concentration and uniformity of concentration were made by performing microharness surveys across the gage diameter of untested specimens. The maximum variation of concentration across a gage was held within ± 5% of the average composition.

Tensile testing was done on an Instron TT-D testing machine equipped with a furnace and a gas-tight testing jig. High purity zirconium chip gettered argon was passed through the testing jig to prevent surface oxidation of the tensile specimen.

Work hardening, flow stress and elongation data were reduced directly from

load-displacement curves, while the reduction in area was computed by using a low power microscope fitted with a moving micrometer eyepiece. Each fracture surface was modeled as an ellipse requiring two orthogonal diameters to be measured for each fracture surface and the final area computed.

SEM photomicrographs were made on a Cambridge Mark II, or on a JSM 3Sc scanning electron microscope which is a recent acquisition in this department.

Experimental Results

Tensile testing was performed between 300 and 1000 K at three strain-rates (8.3×10^{-4}, 8.3×10^{-5} and $8.3 \times 10^{-6} s^{-1}$). Testing at the slowest strain-rate ($8.3 \times 10^{-6} s^{-1}$) remains unfinished and will be completed during the coming year. The data for these tests are summarized in Figs. 3, 4 and 5.

Fig. 3 shows the difference between the flow stress at 0.05 and 0.002 strain, as a function of the testing temperature for the strain-rates investigated. This variable is indicative of the work hardening over this strain range. Several features can be noted in this plot. The work hardening behavior shows two definite peaks within this temperature range. This is probably also the case at the slowest strain-rate although additional tests will be required to show this unambiguously.

The effect of the strain-rate on these work hardening peaks can also be seen in this figure. By reducing the strain-rate, the peaks are generally increased in magnitude and shifted toward lower temperatures in a manner consistent with an Arrenhius relationship. Using this last observation, it is possible to obtain activation enthalpies characteristic of these peaks by fitting the peak temperatures to an Arrenhius equation. This calculation gives activation

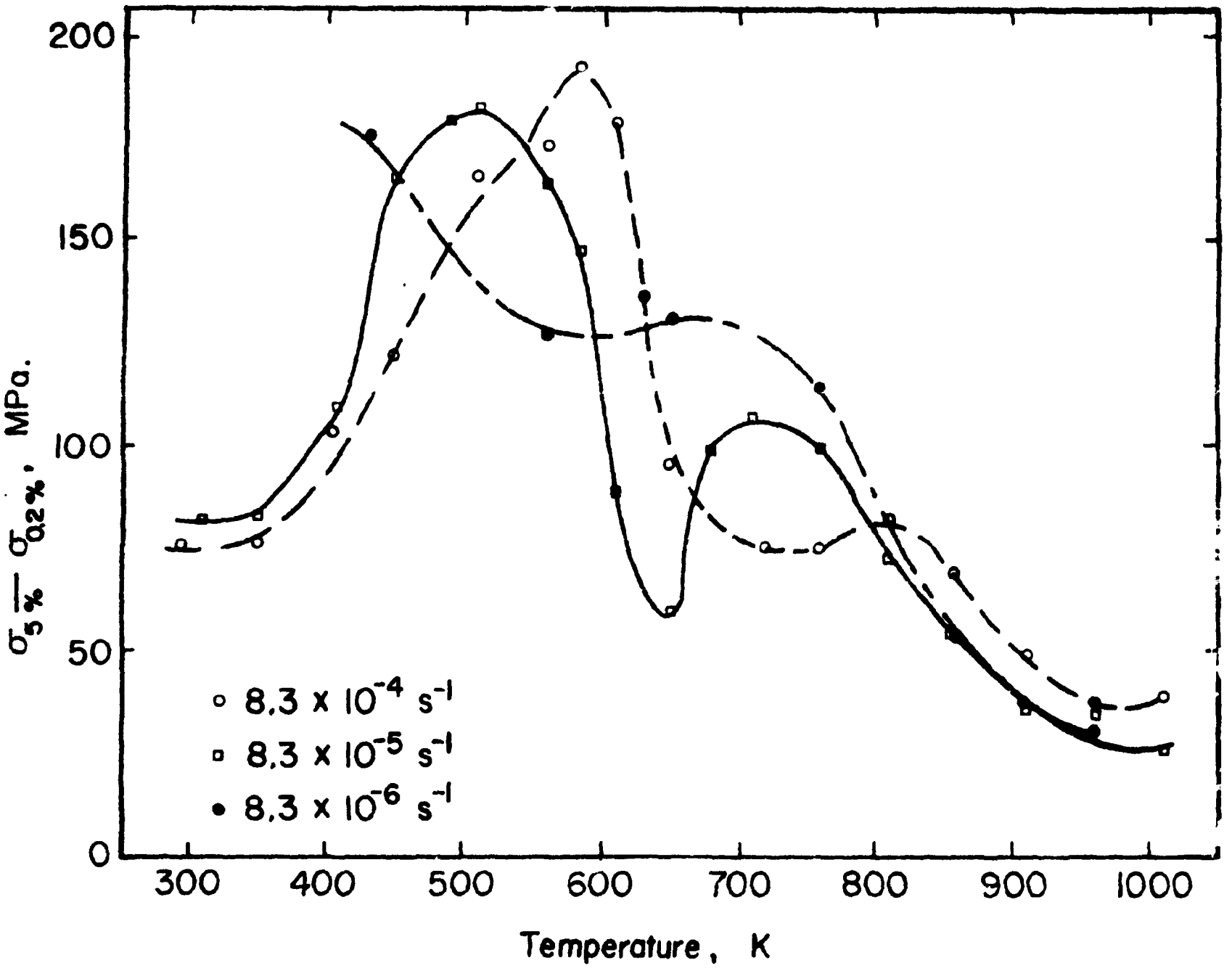

Figure 3. The increase in flow stress between 5% - 0.2% strain as a function of the test temperature for three strain-rates.

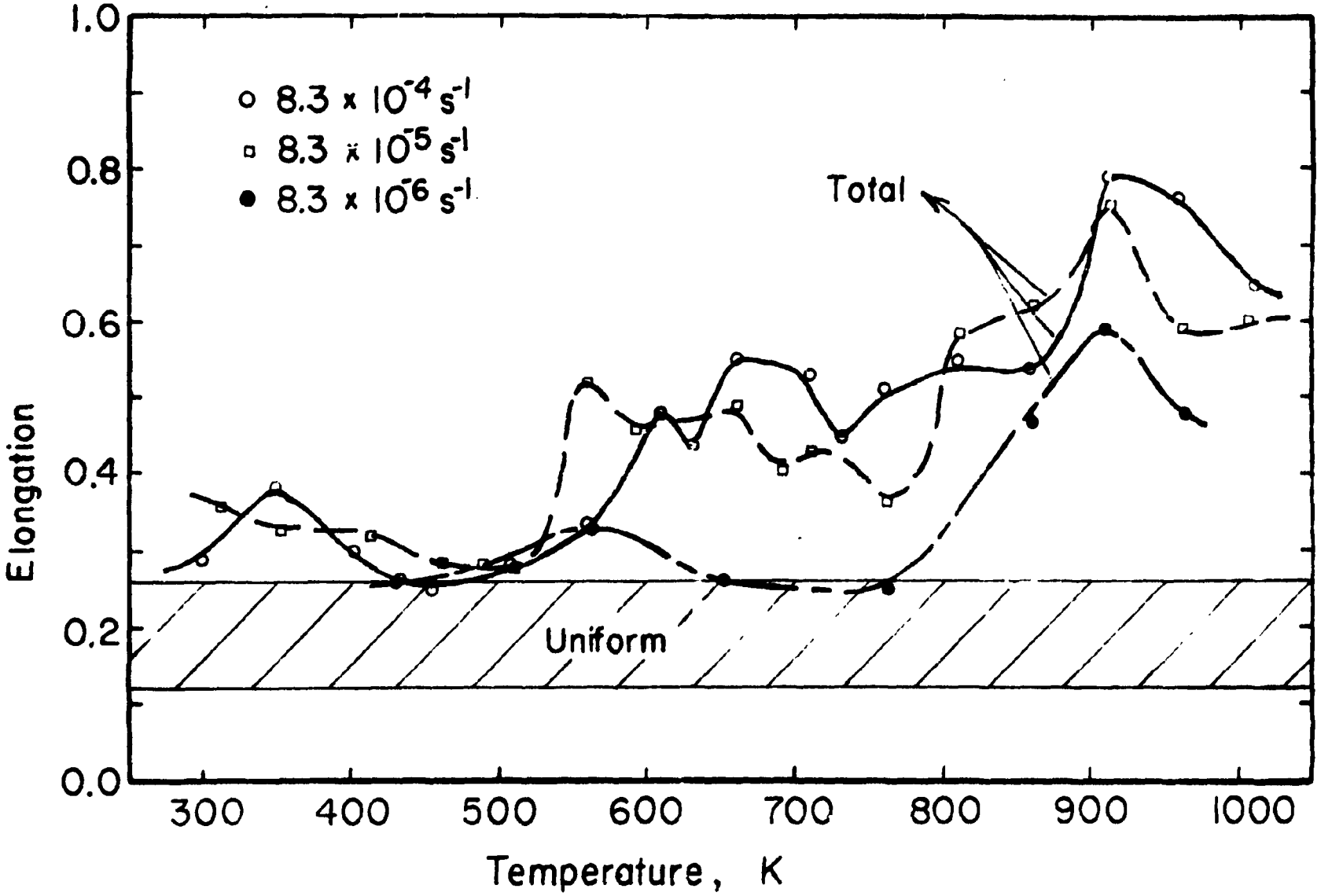

Figure 4. The total elongation as a function of test temperature for three strain-rates. The range of uniform elongation at all strain-rates is indicated by the shaded region.

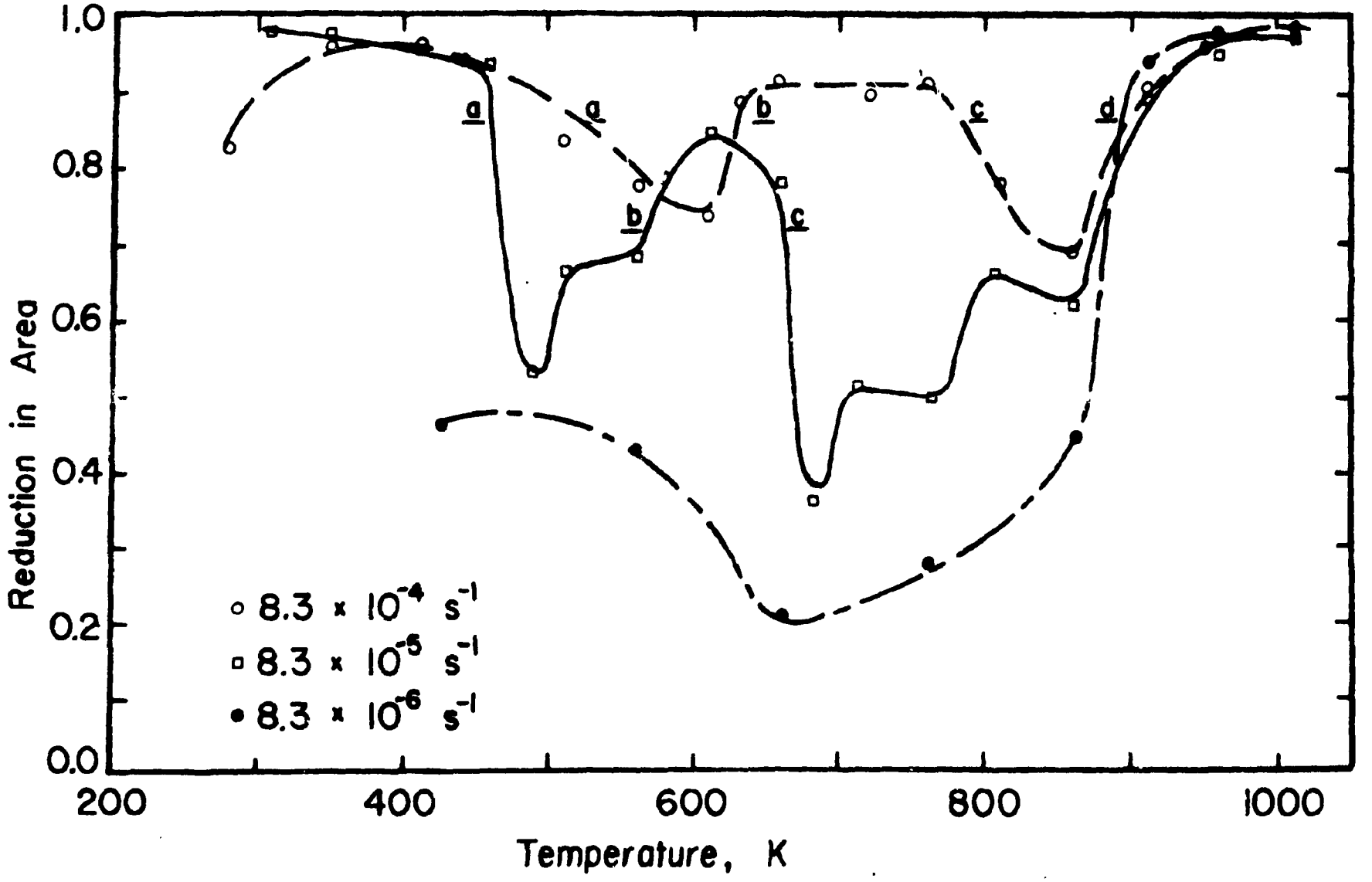

Figure 5. The reduction-in-area as a function of test temperature for three strain-rates.

enthalpies of roughly 27 kca /mole for both peaks. While this value is in good agreement with the enthalpy for diffusion of oxygen in niobium, it appears unlikely that both peaks are associated with this interstitial. A more reasonable interpretation, suggested by activation enthalpies derived from the data of Wessel et al.,[10] is that the lower temperature peak is associated with oxygen and the higher temperature peak with nitrogen. A better value for these enthalpies should be available when testing at the slowest strain-rate is completed.

Fig. 4 shows the variation of total elongation as a function of test temperature for the three strain-rates. To avoid unnecessary clutter, the uniform elongations are indicated on the plot by the shaded area. At each strain-rate, there appear two regions where the total elongation increases sharply in a feature characteristic of the "blue brittle effect" found in dynamic strain-aging regimes. This interpretation is further supported by noting that these features appear to be associated with the work hardening peaks of Fig. 3, both in the temperatures where they occur and in the corresponding temperature shifts induced by strain-rate changes. Thus, Figs. 3 and 4 indicate that dynamic strain-aging is occurring in the two regimes associated with the work hardening peaks and the blue brittle effect. This should be considered when examining the extent of the embrittlement described in the reduction-in-area data discussed below.

When examining embrittlement phenomena, the elongation, uniform or total, can often be a misleading parameter due to features such as blue brittleness which is primarily a phenomenon associated with necking. A more informative approach to characterizing the embrittlement phenomena is to observe both the

reduction-in-area and the fracture morphology as a function of the testing temperature, strain-rate and interstitial concentration. During the last year a start on this type of analysis was made. The reduction-in-area as a function of the test temperature for three strain-rates is presented in Fig. 5. This plot shows two minima at the fastest strain-rate. These increase in magnitude and extent as the strain-rate is decreased until, at the slowest strain-rate, the distinction between the two minima disappears. In addition, it can be noted that three of the four reduction-in-area transitions (labeled a, b and c) are visibly shifted by a change in strain-rate. Thus, it will be possible with more refined data to determine whether these shifts can be characterized by Arrenhius relations and thus to obtain the corresponding activation energies. The high temperature transition (d), on the other hand, displays no visible shift for a strain-rate change factor of 100. This would imply that if strain-rate is a factor in the position of this transition, then it must be characterized by a very large activation energy such as that for recovery (self-diffusion in niobium $\sim$ 100 kcal/mole).

Fracture Morphology

The fracture mode changes in a complex manner as the testing temperature and strain-rate are varied. This behavior is indicated in the schematic plot of Fig. 6 which shows regions of fracture mode predominance superimposed on the reduction-in-area curves for each of the strain-rates.

At the fastest strain-rate the fracture mode varies from microvoid coalescence (MVC) to MVC with external cracking, and then back to MVC. It should be noted that although two minima exist at this strain-rate, only one transition in

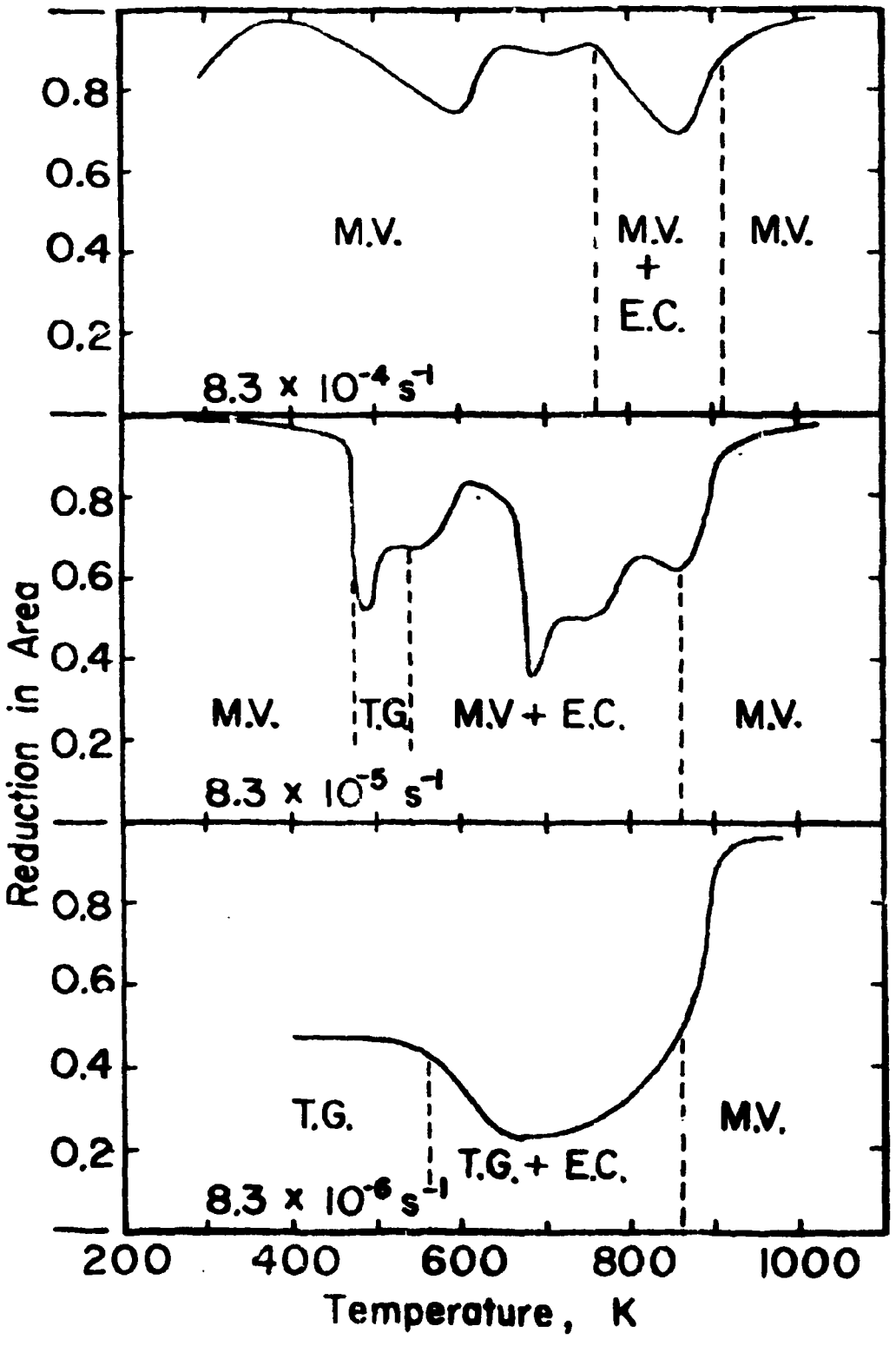

Figure 6. Region of fracture feature predominance superimposed on the reduction-in-area data curves. M.V. - microvoids, E.C. - external cracking, T.G. - transgranular. The results for three strain-rates are shown.

fracture mode occurs, within the higher temperature minimum where external cracking begins to contribute to the final fracture area. In the region of the lower minimum, however, no transition in fracture mode is observed suggesting that the mechanism responsible for this ductility minimum depends on the internal mechanical variables at this temperature and strain-rate rather than on the initiation of a particular fracture mode. This raises the possibility that the higher temperature minimum may not be directly related to the external cracking that occurs over the same temperature range, but simply coexists with this cracking.

At the intermediate strain-rate the two minima have increased in magnitude and extent, but remain distinct. In addition, a number of changes of fracture mode occur as the tests proceed from 300 to 1000 K. A new feature is introduced within the lower temperature minimum as the fracture mode changes to transgranular fracture over a temperature range of about 80 K. Fig. 7 is a photomicrograph of a specimen tested within this region. From this figure several features become apparent. First, the presence of cleavage steps and river patterns indicate that the fracture mode has a quasi-cleavage form as opposed to the more general transgranular form. In addition, the cleavage facets appear to be of roughly the same size as the grains in the material ($\sim$ 70 μm) with large steps separating the facets indicating that crack fronts likely pass through a single grain and stop. Finally, the facets in the foreground of Fig. 7 show considerable curvature. This implies that the material was deformed extensively prior to crack initiation. This observation is supported by Fig. 8 which is of a specimen tested identically to that of Fig. 7 except that the test was stopped after necking and prior to failure. It was then sectioned longitudinally, polished

BLANK PAGE

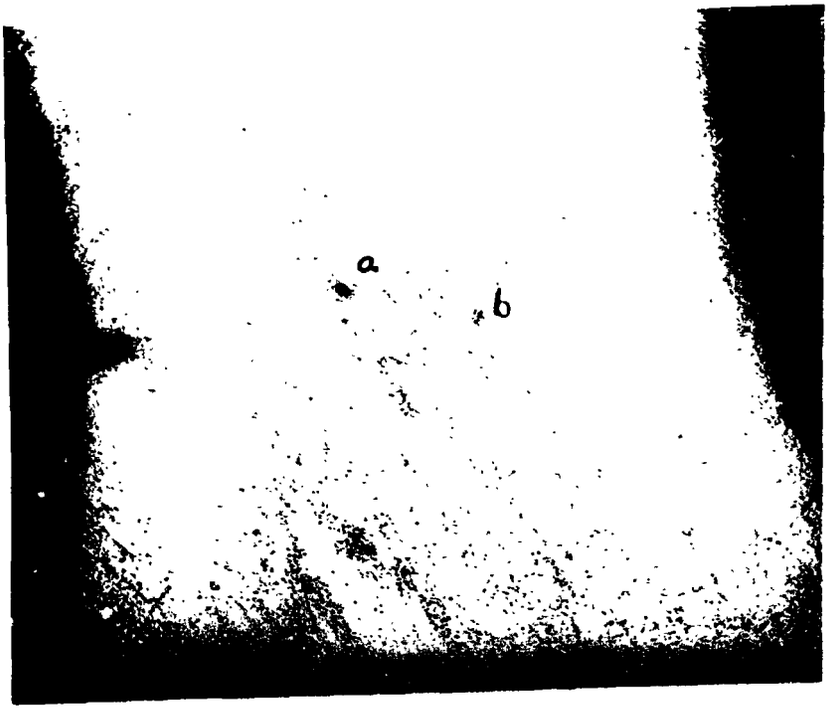

Figure 8. Photomicrograph of a tensile specimen, tested under conditions identical to those of Fig. 7, and unloaded prior to failure. It was then longitudinally sectioned and polished. Two pores were observed and are marked (a) and (b). The surface notch is a reference mark. 60 X

BLANK PAGE

and etched. This revealed only two major pores near the specimen's center indicating that at this late stage in deformation crack initiation had not yet occurred. In the high temperature minimum, at the intermediate strain-rate, extensive surface cracking occurred. A typical surface crack site is shown in Fig. 9. Here it can be seen that near the surface of the tensile specimen (LHS of the figure) the crack has propagated intergranularly. The propagation mode changed after the crack had moved several grains deep into the specimen. At this point the mode becomes transgranular while showing none of the cleavage steps or river patterns characteristic of the quasi-cleavage features of the low temperature minimum. This is possibly because in this situation, the crack is propagating into a series of grains across a broad front many grains wide, rather than being re-nucleated at each successive, grain boundary.

The slowest strain-rate differs in that apparently only one ductility minimum exists extending from below 400 K to ~ 850 K. Morphologically no new fracture modes appear at this strain-rate. The fracture mode for these tests appears to result from a competition between internally nucleated quasi-cleavage cracks and external cracks propagating inward from the gage surface. Over the embrittlement region there is little or no evidence for MVC failure even in the interior of the tensile specimen.

In the past year a survey of the embrittlement regime found in oxygen doped niobium was instituted. It is felt that this has confirmed the embrittlement phenomenon to be physically similar to slow strain-rate embrittlement due to hydrogen which occurs in BCC metals at low temperatures. In addition, it is believed that these data support a connection between the phenomena of slow strain-rate embrittlement phenomenon and of dynamic strain-aging.

DISCUSSION - The results of Task I obtained in the past year are discussed in Section B1 - Task 1 on page 5.

Figure 9. Photomicrograph of the fracture surface of a tensile specimen pulled to failure at 762 K near the upper temperature ductility minimum at a strain-rate of $8.3 \times 10^{-5} s^{-1}$. The edge of the fracture surface is at the LHS of the figure. 300 X

C. Discussion of Progress on Task II

Introduction

Strain-aging in a BCC metal such as vanadium involving the interaction between interstitial atoms and dislocations appears to involve at least two mechanisms. At short aging times, interstitial atoms respond to the stress field of a dislocation by ordering. This process, called Snoek ordering, involves only one or two interstitial atom jumps. With longer aging times, interstitial atoms diffuse to the dislocation from positions many atom jumps away and condense in an atmosphere about the dislocation. This is referred to as Cottrell aging.

While much research has been done on Cottrell aging, relatively little work has been done on Snoek aging. In particular the role of the magnitude of the applied stress, while known to be important, has not been elucidated.

The primary parameter used to study both Snoek and Cottrell aging is the magnitude of the return of the yield point. Determination of this parameter involves loading a specimen to a particular strain at a particular temperature, unloading it and allowing it to age, then reloading it and measuring the magnitude of the yield point return.

These tests usually refer to the aging as being "static" where a primary assumption is that dislocations are not mobile during the aging process. The results of this investigation are not in complete agreement with this assumption. If the specimen is aged under stress it is found that dislocations are mobile. and the velocity at which they move is controlled by the magnitude of the stress during aging.

This investigation seeks to determine the role of applied stress in the aging process occurring by a Snoek ordering mechanism.

Experimental Procedure

VP grade vanadium, 99.9% pure in the form of 12.7 mm diameter rod was obtained from the Materials Research Corporation. According to the manufacturer it contained in wt. ppm: C - 15, O - 220, H - 6 and N - 35.

The rod was swaged to a diameter of 4.75 mm and cylindrical tensile specimens were machined having a gage length of 12.7 mm and a gage section diameter of 3.18 mm. The specimens were annealed at 1373 K for 1 hour to yield a uniform grain size of 60 μm. Another set of specimens were annealed at 1273 K for 1 hour. Metallographic examination indicated that these specimens were not fully recrystallized.

Tension tests were conducted on an Instron in an oil bath maintained to within ± 0.5 K at 353 and 363 K. The specimens were loaded to a prestrain of ∿ 9% at a strain-rate of $6.7 \times 10^{-5} s^{-1}$. They were then unloaded to stress levels between 10% - 98% of the flow stress at 9% ε and aged under load for times ranging from 5 minutes to 10 hours.

It was possible to maintain the stress (load) to within < 0.5% of the prestrain flow stress (load) by utilizing an electronically controlled feedback loop between the strip chart and the cross head. The procedure used allows the desired load for aging to be preset at the beginning of the test. The specimen is prestrained to 9% ε and unloaded. When the preset aging load is reached the cross head automatically begins reloading the specimen. It will continue loading to a preset value as small as 2 lbs. above the load which causes the cross head

to begin loading. The cross head movement then stops until the specimen has relaxed down to the preset aging load and the cycle is repeated.

There are a number of advantages to this form of aging, as compared to a test where one merely relaxes the specimen for the duration of aging, the technique largely used by others in the past. Fig. 10 illustrates the primary difference. In the relaxation method, the stress is not maintained at a constant level but falls progressively with time though a wide range. In the present method the stress can be held to within ± 0.5% of the aging stress for the entire aging period. This is a critical difference due to the dramatic effect of aging stress on the aging process.

Another advantage to this method of testing is that it is possible to measure both the amount of strain and the strain-rate during aging. This may be understood with reference to Fig. 10 which shows the shape of the load-time relationship during aging. In a cycle such as defined by points a, b and c, the specimen deforms plastically between points a and b while the load relaxes. The machine then reloads the specimen rapidly between points b and c. During the reloading interval between points b and c the strain can be considered elastic. With the aid of measurements of the magnitude of the load increment and the combined spring constant of the machine and specimen a calculation of this elastic increment of strain can be made. This increment of elastic strain is then assumed to be equal to the plastic strain increment that occurs during the relaxation portion of the cycle from point a to b. The total strain for the complete aging period is then taken equal to the strain per load drop times the number of load drops. The strain-rate at any time during aging can be evaluated by dividing a strain increment by the time increment required to relax the load (Fig. 10).

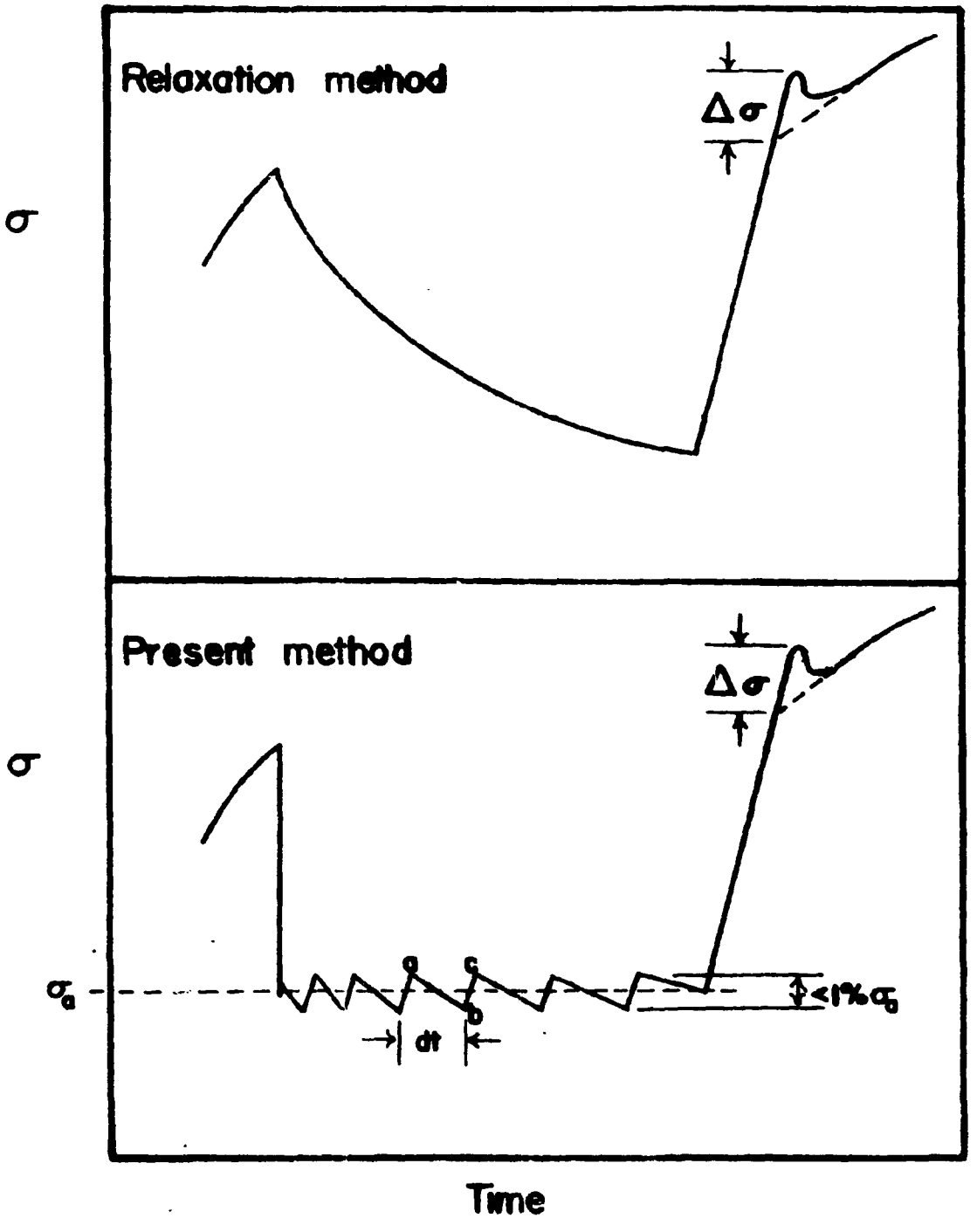

Figure 10. Comparison between the relaxation method and the present method of applying the aging stress. In the relaxation method the stress falls continuously with time. In the present method the stress can be held to within < 0.5% of the aging stress.

The return of the yield point is measured by the extrapolation method (see Fig. 10) applied to the test chart. The Instron machine's stepped zero suppression is used for optimum accuracy. The extrapolation method effectively eliminates from consideration the work hardening that occurs during aging under stress. This has been confirmed by estimating the amount of work hardening during aging in terms of the strain developed during the aging period and the average work hardening rate based on the work hardening rate before and after aging.

Results

The return of the yield point, $\Delta\sigma$, for a specimen aged at 353 K at 92% of the flow stress is plotted against aging time in Fig. 11. The characteristic behavior observed in this curve can be divided into 3 sections. In regions A and C, the yield point return increases steadily with time. In region B, the effect of aging time on the yield point return appears to level off as a plateau. This plateau has been determined by other investigators[11-13] to correspond to the maximum of the aging due to Snoek ordering. The rise in the curve after the plateau is due to Cottrell aging. The effect of temperature on the form of the $\Delta\sigma$ versus time curve is shown in Fig. 12. The data used to plot the curve for the 363 K tests was obtained from specimens of a different grain structure and can only be used for a qualitative comparison. It is seen that at the higher temperature less aging time is required for the plateau to be observed and that the total magnitude of the yield point return in this plateau is lower than that for the lower temperature. This result is in agreement with the observations of others.[11,12]

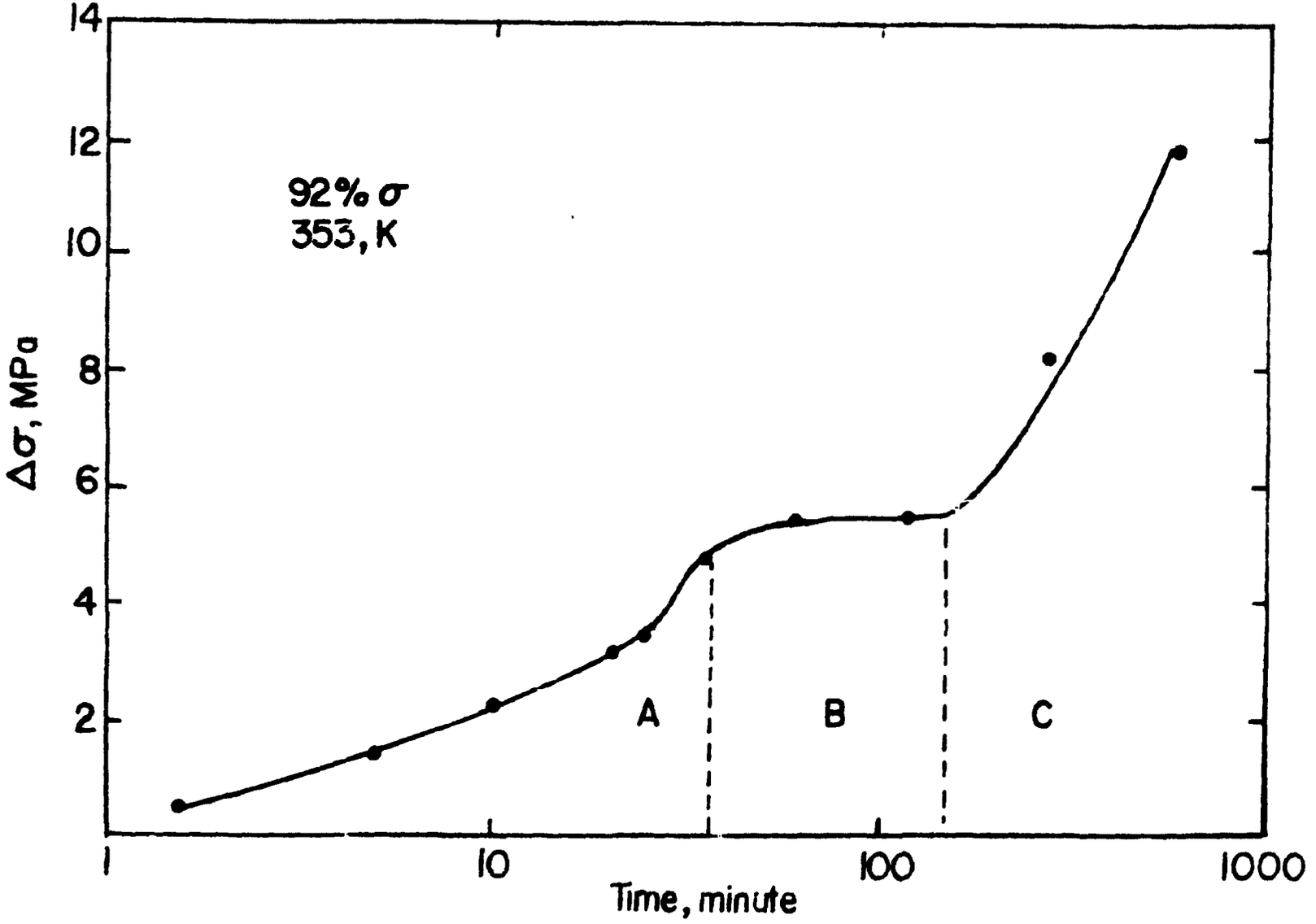

Figure 11. Yield point return versus aging time for a specimen aged at 353 K at 92% of the flow stress. Region A corresponds to Snoek aging. The plateau delineated as region B corresponds to maximum aging due to Snoek ordering. Region C is associated with Cottrell aging.

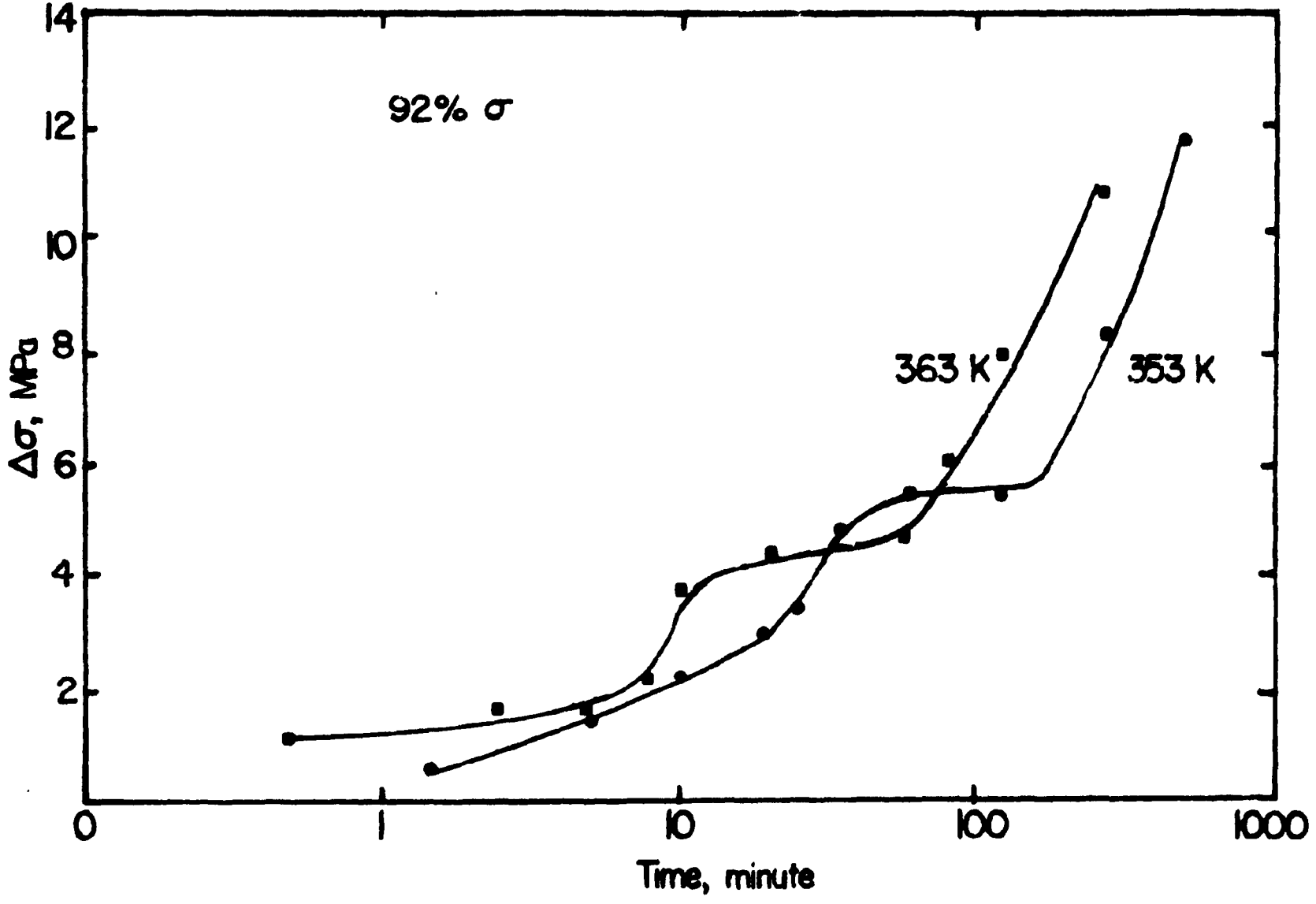

Figure 12. Yield point return curves corresponding to two aging temperatures, 353 and 363 K.

The effect of stress on the magnitude of the yield point return in specimens aged at 353 K for 5 minutes at stress levels ranging from 10% to 98% of the flow stress is shown in Fig. 13. It is seen that increasing the magnitude of the aging stress (% flow stress) causes a climb in the magnitude of the yield point return from a value of 1.7 MPa at 10% σ_f to almost 4.8 MPa at 92% with the most rapid rise in the yield point return occurring between 86 and 92% σ_f. A maximum yield point return is observed at 92% of the flow stress with a very sharp drop off at higher aging stresses.

It can be seen in Fig. 14 that an increase in yield point return with increasing aging stress appears for all aging times investigated.

Preliminary tests indicate that there may be a finite unloading yield point effect. This would imply that at the lower aging stress levels a finite portion of the observed yield point return may be due to an unloading yield point return like that first investigated by Haasen and Kelly.[5]

DISCUSSION - The results of this task obtained in the past year have been discussed and summarized in Section A3 on page 2 (Result of Major Significance) and Section B1 - Task II on page 7 (Objectives and Salient progress).

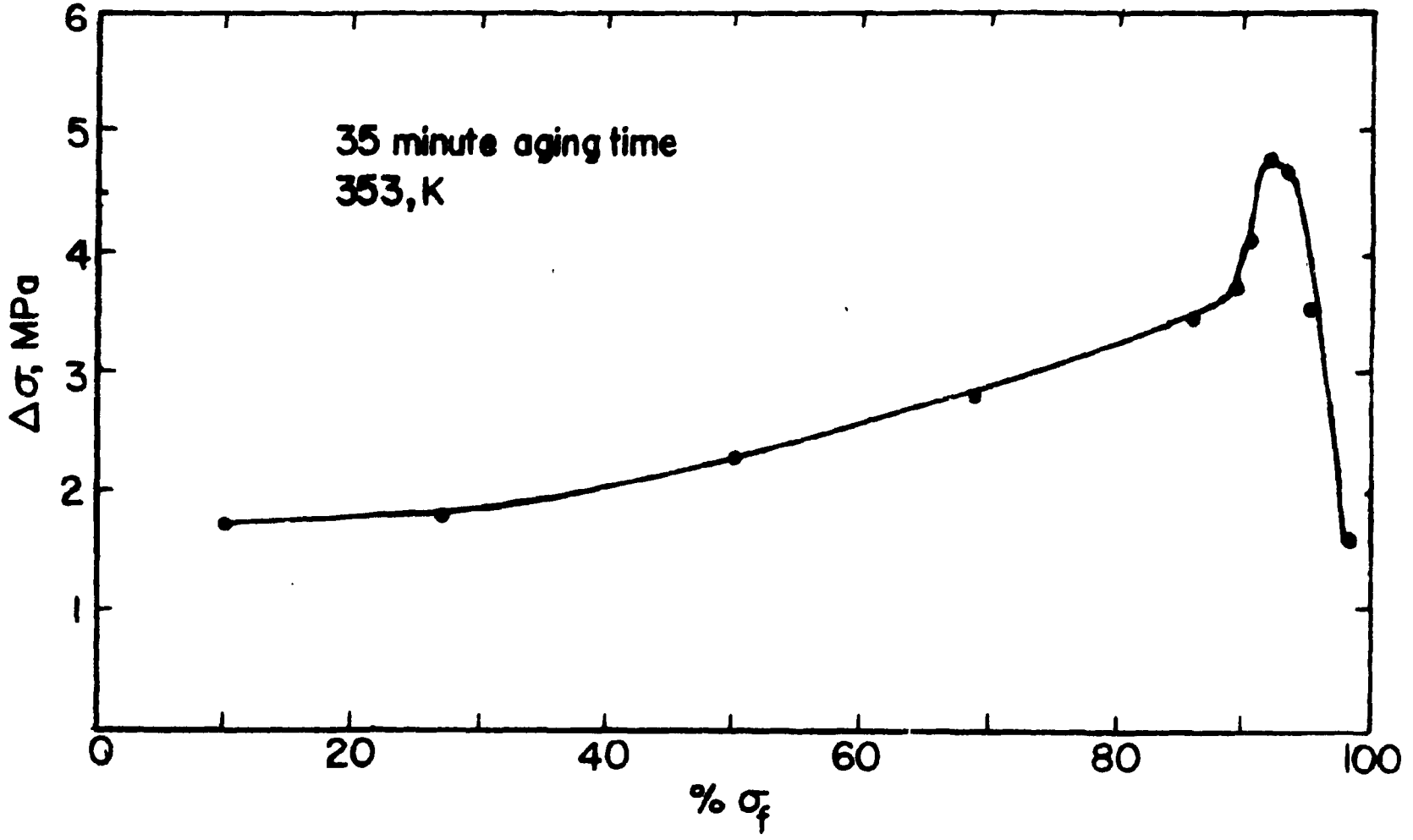

Figure 13. Effect of stress on the yield point return observed for a constant aging time, 35 minutes. Stress levels range from 10% to 98% of the flow stress.

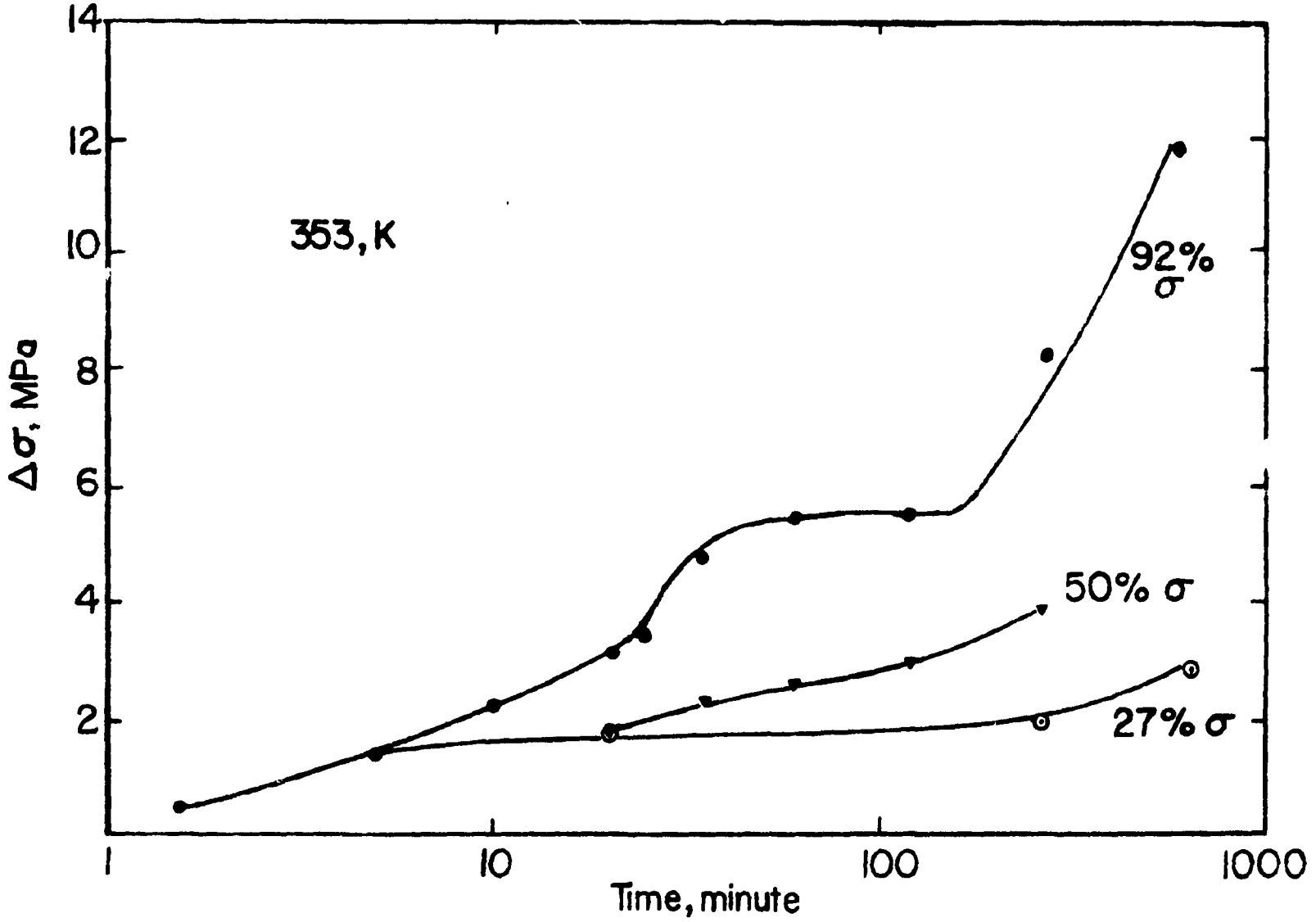

Figure 14. Effect of stress on the yield point return. An increase in the yield point return is observed with increasing aging stress for all the times examined.

REFERENCES

1. E. A. Almond and D. Hull, Phil. Mag., 1966, vol. 14, pp. 515-529.

2. G. F. Bolling, Phil. Mag., 1959, vol. 4, pp. 537-559.

3. A. N. Holden and F. W. Kunz, J. Appl. Phys., 1952, vol. 23, p. 799.

4. J. O. Brittain and S. E. Bronisz, Trans. AIME, 1960, vol. 218, pp. 289-294.

5. P. Haasen and A. Kelly, Acta Met., 1957, vol. 5, pp. 192-199.

6. J. R. Donoso and R. F. Reed-Hill, Met. Trans. A, 1976, vol. 7A, pp. 961-965.

7. G. Schoeck and A. Seeger, Acta Met., 1959, vol. 7, pp. 469-477.

8. A. H. Cottrell and B. A. Bilby, Proc. Phys. Soc., 1949, vol. A62, pp. 49-62.

9. S. A. Bradford and O. N. Carlson, Trans. AIME, 1962, vol. 224, pp. 738-742.

10. E. T. Wessel, L. L. France and R. T. Begley, Columbian Metallurgy, AIME, Met. Soc. Conf., vol. 10, pp. 459-502, Interscience, New York, 1961.

11. Y. Nakada and A. S. Keh, Acta Met., 1967, vol. 15, pp. 879-883.

12. P. Delobelle, C. Oytana and D. Varchon, Mat. Sci. and Engr., 1977, vol. 29, pp. 261-269.

13. D. V. Wilson, B. Russell and J. D. Eshelby, Acta Met., 1959, vol. 7. pp. 628-631.